



Cite this: *Dalton Trans.*, 2018, 47, 16255

Group 10 metal–thiocatecholate capped magnesium phthalocyanines – coupling chromophore and electron donor/acceptor entities and its impact on sulfur induced red-shifts†‡

Malcolm Alan Bartlett^{a,b} and Jörg Sundermeyer^{id} *^{a,b}

A new and facile method of generating thiolate groups at the phthalocyanine (Pc) β -position is presented as well the unique properties that these groups confer on the Pc ligand upon coordination of group 10 metals Ni, Pd and Pt(dppe) or SnMe_3 . In particular, the Q-band is shifted to almost 800 nm for all group 10 metals used, and the complexes show panchromatic absorption owing to new absorbance bands that appear between 400 and 650 nm. Enhanced intersystem-crossing for all transition metal coordinated Mg(Pc) complexes was demonstrated by the moderate to very high singlet oxygen quantum yields of 0.36, 0.76 and 0.91 for the Ni, Pd and Pt coordinating complexes, respectively, which show that the heavy metals have direct influence on the Pc π -system and inter-system-crossing (ISC). This was further confirmed by MO calculations, which show mixing of metal and ligand orbitals, as well as suggest that the Q-band transition has both $\pi \rightarrow \pi^*$ and ligand-to-metal charge transfer characteristics. Furthermore, the origin of the Q-band red-shift was shown to be due to greater destabilization of the HOMO compared to LUMO/LUMO+1, thus decreasing the HOMO–LUMO band gap.

Received 11th September 2018,
Accepted 16th October 2018

DOI: 10.1039/c8dt03681k

rsc.li/dalton

1. Introduction

Heteroleptic complexes, where one of the ligands binds a metal *via* a thiolate group, have relevance for energy conversion in dye-sensitized solar cells¹ or for energy storage, *e.g.* water splitting,² or the reduction of H^+ to H_2 .^{3d} In these applications, the thiolato or endithiolato ligand is often an electron donor, and the process can be driven either photo- or electrochemically.³ It is therefore desirable that such ligands have both good electron-donating and, for photo-driven processes, good light absorbing properties. Examples of such endithiolato or dithiocatecholato ligands with extended π -systems ranging from simple maleonitrile⁴ and benzene^{3d,5} groups to BODIPY⁶ derivatives can be found in the literature; some representative examples are shown in Fig. 1.

Phthalocyanines (Pcs) are known for their strong light absorbing properties as well as general chemical and physical stabilities.⁷ Consequently their application in optoelectronic devices, such as near-infrared (NIR) imagers and dye-sensitized-solar-cells, continues to be extensively investigated.⁸ In particular, increasing the light absorption of Pc and promoting charge transfer to an acceptor moiety^{9,10} is a topical area of research, as this would enable a more efficient utilization of the full solar spectrum and more efficient photo-driven processes. Many strategies have been employed to improve light harvesting, such as incorporating additional chromophores into the Pc to create a donor with absorbance between the B- and Q-bands to create a so-called panchromatic-absorber.^{11–14}

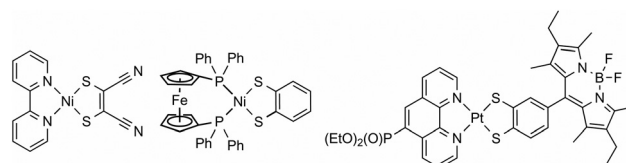


Fig. 1 Heteroleptic complexes employing a dithiolate-containing ligand as a donor ligand for photo- or electrochemically active intermolecular charge transfer: $[(\text{dtmn})\text{Ni}(\text{bpy})]$,⁴ $[\text{Ni}(\text{bdt})(\text{dppf})]$ ^{3d} and a $[(\text{BODIPY})\text{Pt}(\text{phen})]$ ⁶ derivative.

^aDepartment of Chemistry, Philipps-Universität Marburg, Hans-Meerwein St 4, 35032 Marburg, Germany

^bWissenschaftliches Zentrum für Materialwissenschaften (WZMW), Marburg, Germany. E-mail: jsu@chemie.uni-marburg.de

† This paper is dedicated to Prof. Wolfgang Sundermeyer, Heidelberg on the occasion of his ninetieth birthday.

‡ Electronic supplementary information (ESI) available: Copies of NMR, FTIR and UV-Vis spectra and MS data. See DOI: 10.1039/c8dt03681k

Additionally, many strategies involve shifting the Q-band absorption maximum to longer wavelengths to harvest NIR light energy. Although it has been known for many years that derivatisation of the Pc ligand at the α and β positions (Fig. 2) with organochalcogenide substituents $-ER$, where $E = S, Se$ and Te , causes a bathochromic (red-) shift of the Q-band, it was only recently demonstrated how strong this effect can be, inducing red-shifts of over 100 nm.^{15,16} This is believed to be due to an increase in the size of the effective π -system, caused by mixing of the valence p-orbital with the macrocycle's π -system. Inclusion of anionic thiolate/thiocatecholates groups $-E^-$ into the Pc scaffold should therefore result in a Pc based chromophore with unique optical properties that is, at the same time, a capable donor in the synthesis of photoactive heteroleptic complexes with good charge-transfer activity.

Despite this, there is only one example of a Pc compound bearing formally anionic thiolate groups.¹⁷ The thiolate salt is generated by cleavage of benzyl thioether groups under harsh conditions of a Birch-type reduction ($Na/NH_3(l)$). There are also a few examples of tetraazaporphyrazine (Pz) complexes bearing formally anionic thiolate groups (Fig. 2 shows the core structure of a Pz compound). These were also generated under the same Birch-type conditions.¹⁸ So far, the high temperatures and the use of super-bases, *e.g.* DBU, often associated with Pc or Pz ring formation preclude the use of ideal thiolate protecting groups, which later on are readily cleaved under mild conditions.¹⁹ To date, there has been no convincing alternative but to mask the thiolate as a robust PcS-benzyl functionality, followed by cyclisation of dinitrile and deprotection of the resulting dye-benzylthioether under extremely harsh Birch conditions not compatible with the goal of trapping sodium thiolate *in statu nascendi* with a wide range of transition metal complexes. A much milder deprotection strategy would open a multitude of perspectives in using such dyes as thiolate or thiocatecholate ligands in heteronuclear transition metal chemistry.

Here, we present both a new and facile method of generating thiocatecholate groups on the Pc ligand and show how coordination of metals, in particular group 10 metal ions, by these thiocatecholate groups can have a strong influence on the Pc ligand's optoelectronic properties, which are consider-

ably stronger than those observed for thioether substitution. Given the broad range of potential applications of thiol-substituted Pc derivatives, these findings, while broadening the perspectives for coordination chemistry with Pc ligands, have relevance for the design and synthesis of chromophore complexes for photo-driven redox chemistry.

2. Experimental

2.1. Methods and materials

4,5-Dichlorophthalonitrile was prepared from 4,5-dichlorophthalic acid (Sigma Aldrich) according to the literature procedures.²⁰ 1,3-Dihydro-2*H*-benzimidazole-2-thione was prepared using the method of Zhivotova *et al.*²¹

Photo-irradiation was performed using a halogen lamp with an adjustable power rating, which was set to 100 W. Light was filtered through a water filter for removal of infrared light and then through a glass filter with a cut-on wavelength of 500 nm. NMR spectra were obtained on a Bruker AVANCE 300 spectrometer. Chemical shifts are reported in δ (ppm) values. ¹H and ¹³C NMR values were referenced to residual solvent as an internal standard, while ¹¹⁹Sn NMR values were referenced to Me₄Sn. The following abbreviations were used: s = singlet, d = doublet, t = triplet, q = quartet, m = multiplet and br = broad singlet. Mass spectra were recorded on a Thermo Fischer Scientific LTQ-FT Ultra, or on a Bruker Biflex III-Spectrometer (MALDI matrix DHB). UV-Vis spectra were recorded on a Varian Cary Eclipse 5000. FTIR spectra were recorded using a Bruker Alpha Platinum ATR single reflection diamond spectrometer.

2.2. Singlet oxygen quantum yields

Singlet oxygen quantum yield measurements were performed using the set-up described above. In a typical measurement, a cuvette was filled with 2 ml of sample solution containing the sensitizer and DPBF, the concentrations of which were such that the absorbance of each was *ca.* 0.2 and *ca.* 1.0, respectively. The samples were saturated with O₂ by bubbling a stream of O₂ gas through the sample solution in the dark for one minute before beginning the measurements under light irradiation. The singlet oxygen quantum yield, Φ_{Δ} , was determined by using the following equation:²²

$$\Phi_{\Delta} = \Phi_{\Delta}^{\text{Std}} (kI_{\text{Abs}}^{\text{Std}}/k^{\text{Std}}I_{\text{Abs}}) \quad (1)$$

where k and k^{Std} are the slopes of the plot of $\ln(A_0/A_t)$ versus time, for the sensitizer and standard, respectively, A_0 and A_t are the measure of DPBF absorbance at time "0" and time "t", and I_{Abs} and $I_{\text{Abs}}^{\text{Std}}$ are the rates of light absorption by the sensitizer and standard, respectively, and are determined using the equation:²³

$$I_{\text{Abs}} = \alpha((AP)/N_A) \text{ with } \alpha = 1-10^{-E} \quad (2)$$

where E is the absorbance of the sensitizer at the irradiation wavelength, A is the irradiated area (2.2 cm²), P is the intensity

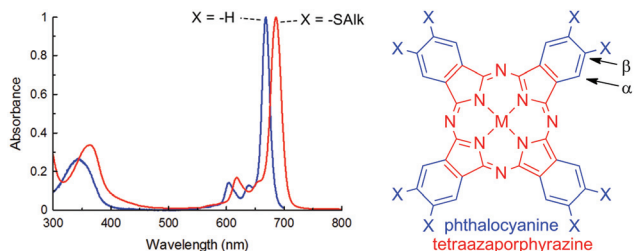


Fig. 2 (left) The typical UV-Vis-NIR absorbance spectra of a metallated Pc ($X = H$) and a Pc derivative with eight thiol groups at the β -positions ($X = SAlk$). (right) The structure of a metallated tetraazaporphyrazine (Pz; red) and phthalocyanine (Pc; blue) with the common positional labelling system for benzene substitution.

of light and N_A is Avogadro's constant. Zn(Pc) was used as a standard ($\Phi_{\Delta} = 0.56$ in DMF).²³

2.3. Molecular orbital calculations

The gas-phase structures of $[(dppeM)_4(S_8PcMg)]$, where M = Ni, Pd or Pt, were optimized at the B3LYP/LanL2DZ level of theory. TDDFT calculations solving for 20 states were then performed at the same level of theory using the gas-phase optimized structures as input structures. All calculations were performed on the MaRC2 computing cluster using the Gaussian09 software package.²⁴

2.4. Syntheses

2.4.1. 4,5-Bis(1-*H*-benzimidazol-2-ylsulfanyl)benzene-1,2-dicarbo-nitrile (dbtpn). 4,5-Dichlorophthalonitrile (2.00 g; 10.15 mmol) and benzimidazole-2-thione (3.20 g; 21.30 mmol) were dissolved in DMF (30 ml). K_2CO_3 (8.5 g; 61.50 mmol) was finely ground before being added to the solution. The resulting suspension was stirred at rt for 18 h. H_2O (80 ml) was then added, causing a yellow solid to precipitate out of solution. The solids were collected by filtration and washed thoroughly with H_2O before being dried *in vacuo*. Mass: 3.75 g. Yield: 87%. 1H NMR (DMSO-*d*₆; 300 MHz, 298 K): δ (ppm) 7.21–7.26 (m, 4H, benz); 7.54–7.59 (m, 4H, benz); 8.19 (s, 2H, phthalonitrile). ^{13}C NMR: (DMSO-*d*₆; 75 MHz; 298 K): δ (ppm) 143.11; 149.54; 135.66; 122.60; 115.22; 113.91. HRMS (APCI+, MeOH): calcd for $C_{22}H_{12}N_6S_2 [M + H]^+$: 425.0639; found: 425.0638.

2.4.2. 4,5-Bis(1-methyl-benzimidazol-2-ylsulfanyl)benzene-1,2-dicarbonitrile (Dmbtpn). Dbtpn (0.25 g; 0.59 mmol) was dissolved in DMF (10 ml). Crushed KOH pellets (0.35 g; 6.25 mmol) were added to this solution, which was stirred for 5 min at rt. MeI (0.8 ml; 2.5 mmol) was added, and stirring was continued for 10 min. H_2O (30 ml) was added, and the precipitate that formed was collected by filtration and washed thoroughly with H_2O . The solids were extracted into $CHCl_3$, dried over $MgSO_4$ and the solvent was evaporated to leave a white crystalline solid. Mass obtained: 0.23 g. Yield: 85%. 1H NMR (300 MHz, DMSO-*d*₆): δ (ppm) 3.82 (s, 6H, $-CH_3$); 7.26–7.38 (dt, 4H, Ar); 7.63–7.69 (t, 4H, Ar); 7.93 (s, 2H, phthalonitrile). ^{13}C NMR (75 MHz, DMSO-*d*₆): δ (ppm) 30.85 ($-CH_3$); 110.92, 114.04, 115.05, 119.04, 122.44, 123.37, 134.96, 136.58, 140.36, 142.80, 143.77. HRMS (APCI+, MeOH): calcd for $C_{24}H_{17}N_6S_2 [M + H]^+$: 453.0951; found: 453.0952.

2.4.3. Magnesium(2,3,9,10,16,17,23,24-octa(1-*H*-benzimidazol-2-ylsulfanyl)-phthalocyanine) $[(RS)_8PcMg]$. Dbtpn (0.800 g; 1.88 mmol) was mixed with $Mg(OEt)_2$ (0.200 g; 1.75 mmol) under N_2 . 1-Octanol (3 ml) was then added to the mixture, which was then homogenised in an ultrasound bath for 15 min. The suspension was then heated at 160 °C for 10 min to afford a dark green solid. This was then cooled to rt before washing with hexane, $CHCl_3$, EtOH and H_2O . Mass: 0.602 g. Yield: 74%. 1H NMR (DMSO-*d*₆; 300 MHz): δ (ppm) 9.29 (s, 8H, PcH); 8.15 (s, 6H, NH); 7.52–7.48 (m, 32H, Ar); 7.18–7.14 (m, 32H, Ar). MS (MALDI+, CH_3CN): calcd for $C_{88}H_{49}MgN_{24}S_8 [M + H]^+$: 1723.32; found: 1723.32. UV-Vis

(DMSO): 702 (s), 664 (sh), 628 (s), 368 (s). FTIR: $\nu/cm^{-1} = 1060$ (s), 1265 (s), 1395 (s), 1595 (s), 2850 (s), 2920 (s), 3051 (m).

2.4.4. Magnesium(2,3,9,10,16,17,23,24-octa[(1-methyl-benzimidazol-2-yl)sulfanyl]-phthalocyanine) $[(^{Me}RS)_8PcMg]$. (Method a) $[(RS)_8PcMg]$ (0.700 g; 0.406 mmol) was dissolved in DMF (10 ml). MeI (1 ml) was then added, followed by crushed KOH pellets (0.500 g; 8.911 mmol). The suspension was stirred for 25 min at rt before being added to H_2O (90 ml). The precipitate that formed was collected by filtration and washed thoroughly with H_2O before being dried *in vacuo*.

(Method b) Dmbtpn (1.01 g; 2.21 mmol) was mixed with $Mg(OEt)_2$ (0.48 g; 4.19 mmol) under N_2 . Octanol (10 ml) was added, and the resulting suspension was homogenised using an ultrasound bath. The suspension was then placed in an oil bath preheated to 170 °C for 35 min. The resulting green suspension was allowed to cool before washing the solids with hexane (3 × 40 ml). Washing was repeated using $CHCl_3$, Me_2CO , EtOH and H_2O until all washings were colourless. The remaining dark green solids were then dried to yield the final product. Mass: 0.874 g. Yield: 86% (Method a). Mass: 0.635 g. Yield: 62% (Method b). 1H NMR (DMSO-*d*₆, 300 MHz, 298 K): δ (ppm) = 3.92 (s, 24H, $-CH_3$); 7.05–7.19 (m, 16H, Ar); 7.56–7.54 (m, 16H, Ar); 8.89 (s, 8H, Pc). LRMS (MALDI+, CH_3CN): calcd for $C_{96}H_{64}MgN_{24}S_8 [M]^+$: 1832; found: 1832. UV-Vis (DMSO): $\lambda/nm = 704$ (s), 670 (sh), 632 (s), 375 (s). FTIR: $\nu/cm^{-1} = 1064$ (s), 1277 (s), 1321 (s), 1370 (s), 1396 (s), 1448 (s), 1595 (w), 2920 (w), 3051 (w).

2.4.5. Magnesium(2,3,9,10,16,17,23,24-octa[(1,3-dimethyl-1*H*-benzimidazol-2-yl)sulfanyl]-phthalocyanine octaoidide) $[(^{Me_2}RS)_8PcMg]I_8$. $[(^{Me}RS)_8PcMg]$ (0.800 g; 0.463 mmol) was dissolved in DMF (15 ml). MeI (4 ml; 64.25 mmol) was then added, and the solution was heated at 80 °C for 16 h. The solution was then added to THF (200 ml), and the precipitate was collected by filtration and washed with THF. The sample was cleaned by repeated dissolution in DMF followed by precipitation from THF. Mass: 1.049 g. Yield: 81%. 1H NMR (DMSO-*d*₆, 300 MHz, 298 K): δ (ppm) 4.28 (s, 48H, $-CH_3$); 7.89–7.92 (m, 16H, Ar); 8.23–8.26 (m, 16H, Ar); 9.45 (s, 8H, Pc). UV-Vis (DMSO): $\lambda/nm = 705$ (s), 630 (s), 362 (sh). FTIR: $\nu/cm^{-1} = 1019$ (s), 1079 (m), 1120 (s), 1281 (m), 1393 (s), 1478 (s), 1590 (m), 1699 (s), 2935 (w), 3014 (w), 3283 (w).

2.4.6. Magnesium(2,3,9,10,16,17,23,24-octa[(trimethyltin)sulfanyl]-phthalocyanine) $[(Me_3Sn)_8(S_8PcMg)]$. $[(^{Me_2}RS)_8PcMg]I_8$ (0.100 g; 0.0337 mmol) and K_2CO_3 (0.160 g; 1.158 mmol) were mixed together, and then suspended in degassed H_2O (3 ml). The suspension was gently heated until a purple solution of $K_8[S_8PcMg]$ free of any solids was obtained. This solution was then added to a stirred solution of Me_3SnCl (0.540 g; 0.271 mmol) in degassed $CHCl_3$ (5 ml). The two phases were mixed until the aqueous phase became clear and the organic phase became green. The organic portion was separated, dried over $MgSO_4$ and filtered. Solvents were then removed from the filtrate to afford a dark green solid. This was washed with hexane and EtOH before being dried *in vacuo* (10^{-3} mbar). Mass: 0.0664 g. Yield: 94%. 1H NMR ($CDCl_3$, 300 MHz, 298 K): δ (ppm) 0.667 (s, $-CH_3$). ^{119}Sn NMR (187 MHz, $CDCl_3$, 298 K):

δ (ppm) 173.79. MS (MALDI⁺, CH₂Cl₂): calcd for C₅₃H₇₁MgN₈S₇Sn₇ [M – [SSnMe₃]]⁺: 1906.69; found: 1906.69. UV-Vis (CH₂Cl₂; 298 K) λ /nm: 321, 358 sh, 434, ~645 sh, 663, 699, 732.

2.4.7. General procedure for the synthesis of K₈[S₈PcMg] and its coordination to [M(dppe)]²⁺. [(^{Me}RS)₈PcMg] (0.070 g; 2.4 × 10⁻² mmol) was treated with a solution of KOH (0.05 g; 0.9 mmol) in degassed H₂O (10 ml). Once all solids had dissolved and a blue solution was obtained, it was added dropwise to a concentrated solution of [MCl₂(dppe)] (0.13 mmol) in THF (20 ml) with vigorous stirring. The suspension that formed was then stirred at rt for 18 h. The sample was then diluted with H₂O and centrifuged to collect the solids. The solids were then washed with MeOH, EtOH, Me₂CO and hexane before being extracted into DCM and filtered. Evaporation of the filtrate left the pure compound.

[[dppeNi]₄(S₈PcMg)]. ¹H NMR (DMSO-*d*₆, 300 MHz, 298 K): δ (ppm) 1.35 (s, 16H, –CH₂CH₂–), 7.34–7.94 (m, 80H, Ph), 9.04 (br, 8H, Pc). ³¹P NMR (DMSO-*d*₆, 101 MHz, 298 K): δ (ppm) 30.24. MS (MALDI-TOF): calcd for C₁₃₆H₁₀₅N₈Ni₄P₈S₈ [M + H⁺ – Mg]⁺: 2590.43; found: 2590.55. UV-Vis (DMSO): λ /nm = 770 (s), 700 (sh), 534 (br), 362 (s).

[[dppePd]₄(S₈PcMg)]. ¹H NMR (300 MHz, DMSO-*d*₆, 298 K): δ (ppm) 1.35 (s, 16H, –CH₂CH₂–), 7.53–7.65 (m, 40H, Ph); 7.91–7.97 (m, 40H, Ph); 8.24 (s, 8H, Pc). ³¹P NMR (DMSO-*d*₆, 101 MHz, 298 K): δ (ppm) 53.76. MS (MALDI-TOF): calcd for C₁₃₆H₁₀₅N₈Pd₄P₈S₈ [M + H⁺ – Mg]⁺: 2781.3406; found: 2782.6098. UV-Vis (DMSO): λ /nm = 765 (s), 698 (sh), 580 (br), 468 (br), 354 (s).

[[dppePt]₄(S₈PcMg)]. ¹H NMR (300 MHz, DMSO-*d*₆, 298 K): δ (ppm) 1.24 (s, 16H, –CH₂CH₂–), 7.63 (br, 40H, Ph), 7.98 (br, 40H, Ph), 9.27 (br, 8H, Pc). ³¹P NMR (DMSO-*d*₆, 101 MHz, 298 K): δ (ppm) 48.34 (¹J_{Pt-P} = 1160 Hz). UV-Vis (DMSO): λ /nm = 764 (s), 702 (sh), 559 (br), 473 (br), 360 (s).

2.4.8. (Bis(1,2-diphenylphosphino)ethane)(4,5-dithiolato-phthalo-nitrile)nickel(II) ([Ni(dppe)(dtpn)]). [NiCl₂(dppe)] (0.150 g; 0.28 mmol) was dissolved in CHCl₃ (10 ml) and added to a solution of H₂dtpn (0.054 g; 0.28 mmol) in CHCl₃ (10 ml). Triethylamine (0.035 g; 0.35 mmol) was then added dropwise, and the resulting solution was stirred for 180 min. The solution was concentrated by rotary evaporation and then loaded onto a silica column. The product was then purified by column chromatography (silica/CHCl₃); it elutes as the first coloured band. Solvent was evaporated to afford a pale orange solid. Mass: 0.141 g. Yield: 78%. ¹H NMR (CDCl₃, 300 MHz, 298 K): δ (ppm) 2.43 (d, ¹J = 8.4 Hz, 4H, –CH₂CH₂–), 7.52 (m, 12H, Ph), 7.66 (s, 2H, phthalonitrile), 7.75 (br, 8H, Ph). ¹³C NMR (CDCl₃, 75 MHz, 298 K): 100.89, 101.45, 105.95, 106.35, 125.99, 129.09, 129.16, 129.27, 131.72, 131.88, 133.41, 133.48, 175.06. ³¹P NMR (CDCl₃, 101 MHz, 298 K): 60.05. HRMS (APCI⁺; CH₂Cl₂): calcd for C₃₄H₂₇N₂NiP₂S₂ [M + H]⁺: 647.0439; found: 647.0436.

2.4.9. (Bis(1,2-diphenylphosphino)ethane)(4,5-dithiolato-phthalo-nitrile)palladium(II) ([Pd(dppe)(dtpn)]). [PdCl₂(dppe)] (0.085 g; 0.15 mmol) and H₂dtpn (0.028 g; 0.15 mmol) were suspended in DCM (5 ml). NEt₃ (0.2 ml; 0.15 g; 1.4 mmol) was

added, and the suspension was stirred at rt for 18 h. The solvent was evaporated and the solids remaining were washed with hexane. The product was then purified by column chromatography (silica/DCM), being collected as the major yellow band. Mass: 0.085 g. Yield: 82%. ¹H NMR (CDCl₃, 300 MHz, 298 K): δ (ppm) 2.58 (d, ¹J = 10.52 Hz, 4H, –CH₂CH₂–), 7.46–7.55 (m, 12H, Ph), 7.61 (s, 2H, phthalonitrile), 7.71–7.78 (m, 8H, Ph). ¹³C NMR (CDCl₃, 75 MHz, 298 K): 27.83, 106.34, 117.27, 128.64, 129.24, 129.31, 129.39, 132.08, 133.02, 133.19, 133.26, 133.34, 156.06. ³¹P NMR (CDCl₃, 101 MHz, 298 K): δ (ppm) 53.19. HRMS (APCI⁺; CH₂Cl₂): calcd for C₃₄H₂₇N₂PdP₂S₂ [M + H]⁺: 695.0132; found: 695.0132.

2.4.10. (Bis(1,2-diphenylphosphino)ethane)(4,5-dithiolato-phthalo-nitrile)platinum(II) ([Pt(dppe)(dtpn)]). [PtCl₂(dppe)] (0.074 g; 0.11 mmol) was mixed with H₂dtpn (0.029 g; 0.15 mmol). The mixture was then dissolved in DCM (5 ml) and NEt₃ (0.2 ml; 0.15 g; 1.4 mmol) was added. The solution was then stirred for 22 h at rt. The solvent was evaporated to afford a yellow-brown solid, which was subsequently washed with MeOH. The solids were then dissolved once more in DCM and loaded onto a silica-gel column. The product was eluted as the second colourless band using DCM. Mass: 0.055 g. Yield: 62%. ¹H NMR (CDCl₃, 300 MHz, 298 K): δ (ppm) 2.46–2.62 (m, 4H, –CH₂CH₂–), 7.47–7.52 (m, 12H, Ph and phthalonitrile); 7.73–7.79 (m, 10H, Ph). ¹³C NMR (CDCl₃, 75 MHz, 298 K): δ (ppm) 106.18, 117.05, 128.91, 129.09, 129.11, 129.19, 132.04, 133.33, 133.40, 133.48, 151.36. ³¹P NMR (CDCl₃, 101 MHz, 298 K): δ (ppm) 44.60 (¹J_{Pt,P} = 1399 Hz). HRMS (APCI⁺; CH₂Cl₂): calcd for C₃₄H₂₇N₂PtP₂S₂ [M + H]⁺: 784.0736; found: 784.0735.

2.4.11. Synthesis of 4,5-disulfanylbenzene-1,2-dicarbonitrile (H₂dtpn). To solid dmbtpn (2.00 g; 2.72 mmol) was added solid KOH (0.5 g; 8.9 mmol) and H₂O (5 ml) to give a suspension. This was sonicated for 15 min, or until all solids dissolved, to give a dark yellow solution. The solution was then diluted with H₂O (25 ml) and acidified with HCl (37%, aq) to cause a yellow solid to separate. This solid was extracted with DCM (3 × 10 ml). The DCM fractions were combined, dried (MgSO₄), filtered and the filtrate was evaporated to leave the pure product as a bright yellow solid. Mass: 0.48 g. Yield: 92%. ¹H NMR (300 MHz; DMSO-*d*₆): δ (ppm) 8.60 (s, Ar). ¹³C NMR (75 MHz; DMSO-*d*₆): δ (ppm) 114.5, 114.8, 135.5, 137.5.

3. Results and discussion

3.1. Synthesis

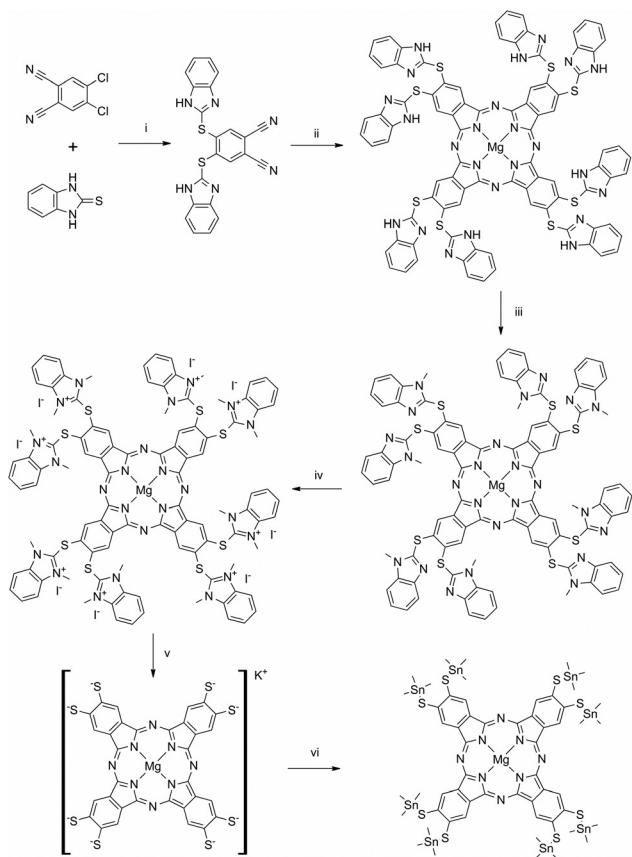
Thiolate protecting groups that can be easily removed are typically not stable under basic conditions, such as those required for phthalocyanine synthesis.¹⁹ We therefore employed a two-step strategy where, first, a stable 2-thio-benzimidazole group was used to introduce a thiol group onto a dinitrile precursor by reacting with readily available 4,5-dichlorophthalonitrile. After normal cyclisation to the Pc dye, a two-fold *N*-methylation leads to benzimidazole-2-thiuronium groups, that are activated for C–S bond cleavage. These are cleaved

with even weakly basic aqueous potassium carbonate to afford an *N,N'*-dimethylbenzimidazole urea derivative as a stable leaving group and a highly reactive and air sensitive potassium thiolate salt $K_8[S_8PcMg]$ for coordination studies.

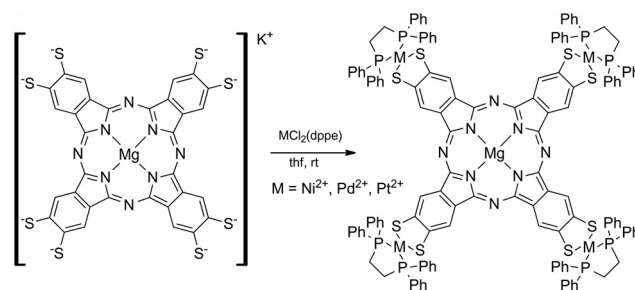
This strategy is demonstrated by the *in situ* synthesis of octathiolato Pc complex $K_8[S_8PcMg]$ and its conversion into Ni, Pd, and Pt(dppe) complexes or trimethylstannanes. Dinitriledithioether was synthesised by the reaction of 4,5-dichlorophthalonitrile with benzimidazole-2-thione in DMF in the presence of K_2CO_3 (Scheme 1). Cyclisation with $Mg(OEt)_2$ in octanol led to the formation of the corresponding octa(2-thiobenzimidazol)phthalocyaninato magnesium complex ($[(RS)_8PcMg]$). Quaternization of the benzimidazole groups was then accomplished *via* two successive *N*-methylations with MeI in DMF, the first one being with the aid of KOH at room temperature and the second one at elevated temperatures. The second *N*-methylation proceeds very slowly at room temperature, with little product formation after several days of stirring. Substitution of the imidazole-H atom with a methyl group can be readily monitored by disappearance of the strong N-H stretching frequency at 2950 and 2850 cm^{-1} in the FTIR spectrum of $[(RS)_8PcMg]$. When quaternisation *via* double methylation of $[(RS)_8PcMg]$ is attempted directly in one step, a by-

product is formed that causes concomitant decomposition of the chromophore, hence the need for a two-step approach. The generated benzimidazolium groups are readily cleaved by KOH (aq) at 0 °C to yield the purple octathiolato Pc complex, $K_8[S_8PcMg]$. Alternatively, this complex can be formed using a milder base, such as K_2CO_3 (aq), at elevated temperatures. $K_8[S_8PcMg]$ is extremely air sensitive, and precipitates from aqueous solution as an insoluble blue-green material when exposed to air. When a THF solution of Me_3SnCl is added to an aqueous solution of $K_8[S_8PcMg]$ in the presence of K_2CO_3 , the Sn-capped complex $[(Me_3Sn)_8(S_8PcMg)]$ forms immediately (Scheme 1). This complex is soluble in common non-polar organic solvents, such as $CHCl_3$. It is a moderately air stable complex, decomposing within days to an unidentified insoluble green compound. The treatment of freshly synthesised $K_8[S_8PcMg]$ with an excess of either Ni-, Pd-, or $[PtCl_2(dppe)]$ gave the tetradiphosphino metal-capped complexes, $[(dppeNi)_4(S_8PcMg)]$, $[(dppePd)_4(S_8PcMg)]$, and $[(dppePt)_4(S_8PcMg)]$ (Scheme 2). It is important though that $K_8[S_8PcMg]$ is added to the dichlorido metal complex, and not *vice versa*, to ensure that the latter is always in excess, or else precipitation of an unknown blue-green solid occurs, which we postulate to be a coordination polymer. The complexes are air-stable in DMSO solutions for days and show no aerobic decomposition in the solid state after several months. They show limited solubility in polar organic solvents, such as DMF and DMSO, as well as in a few non-polar solvents, such as DCM. Because of their insolubility in many common solvents, it is possible to remove excess of $[MCl_2(dppe)]$ or other impurities by washing, and then to extract the product into DCM. Filtration of the extract removes polar impurities to give the pure product as dark purple (Ni) or dark brown (Pd and Pt) solids.

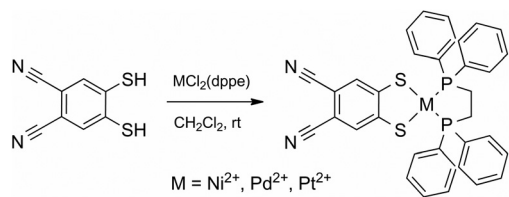
For comparison, smaller heteroleptic complexes of 4,5-dithiolatophthalonitrile ($dtpn^{2-}$) and $[MCl_2(dppe)]$ were prepared. H_2dtpn was synthesised *via* a similar method to that described for the synthesis of $K_8[S_8PcMg]$; namely, 4,5-(benzimidazole-2-thiol)-phthalonitrile was quaternised using methyl iodide by heating in DMF. Unlike $[(RS)_8PcMg]$, both methylations can be performed in a single step by heating the starting dinitrile in a MeI/DMF solution. The benzimidazolium groups were then readily cleaved by KOH in a DMF/ H_2O solution. Neutralization of the solution with HCl (aq) precipitated



Scheme 1 Synthesis of $[(Me_3Sn)_8(S_8PcMg)]$ *via* the octathiolato intermediate $K_8[S_8PcMg]$. (i) K_2CO_3 , DMF, rt; (ii) $Mg(OEt)_2$, 1-octanol, 160 °C, 10 min; (iii) MeI, DMF, rt, 25 min; (iv) MeI, DMF, 80 °C, h, 16 h; (v) KOH (aq), rt or K_2CO_3 (aq), 80 °C; (vi) Me_3SnCl , THF, rt, 5 min.



Scheme 2 Synthesis of group 10 metal-capped complexes $[(dppeM)_4(S_8PcMg)]$.



Scheme 3 Synthesis of heteroleptic dithiocatecholato complexes of group 10 metals for comparison.

H_2dtpn . A solution of H_2dtpn and the desired dichloro metal diphosphine in the presence of an organic base, *e.g.* NEt_3 , gave the corresponding heteroleptic complexes, $[\text{Ni}(\text{dppe})(\text{dtpn})]$, $[\text{Pd}(\text{dppe})(\text{dtpn})]$, and $[\text{Pt}(\text{dppe})(\text{dtpn})]$, in good yield. The general synthesis of these complexes is shown in Scheme 3. The complexes are all air-stable solids that have good solubility in common organic solvents.

3.2. ^{31}P NMR spectroscopy

^{31}P NMR spectra were recorded for the pentanuclear Pc complexes and their mononuclear analogues, as this gives an insight into the M–P and consequently the M–S bonding environment. For the mononuclear $[\text{M}(\text{dtpn})(\text{dppe})]$ complexes, a clear trend in the ^{31}P NMR chemical shifts can be seen, with the signal being shifted downfield in the order $\text{Pt} < \text{Pd} < \text{Ni}$ (Table 1). This trend in shifts appears to follow the trend in size and electropositive characteristic of the metals used. However, this trend in ^{31}P shifts is broken for the pentanuclear complexes, with the order of shifts being $\text{Ni} < \text{Pt} < \text{Pd}$. Furthermore, while the ^{31}P NMR signals are shifted slightly downfield for the Pd- and Pt-capped complexes, the signal for the Ni-capped complex is rather surprisingly shifted by *ca.* 30 ppm up-field compared to the mononuclear analogue. The reason for this remarkable change in ^{31}P NMR shifts caused when a benzene group is replaced by Pc is at present unclear, and will be the subject of further investigation.

3.3. Electronic absorption spectroscopy

All three octa-2-thiobenzimidazole/ium substituted PcMg complexes showed the typical absorption spectra for inner core metallated Pc complexes with eight peripheral thioether groups, with an absorption maximum at *ca.* 700 nm.²⁵ Absorption spectra for these complexes are shown in the ESI.† Of greater interest in this study is the effect that metal coordi-

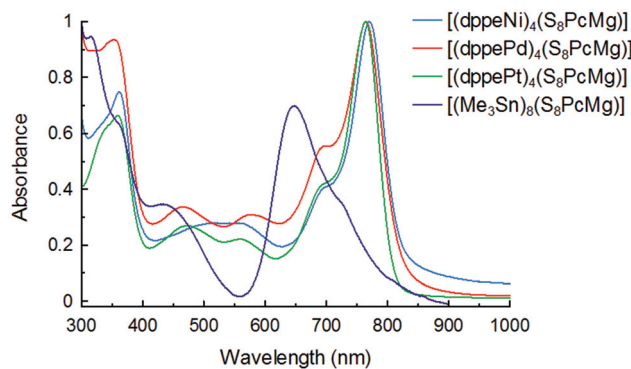


Fig. 3 Normalised absorption spectra of $[(\text{dppeM})_4(\text{S}_8\text{PcMg})]$ ($M = \text{Ni}, \text{Pd}, \text{Pt}$) and $[(\text{Me}_3\text{Sn})_8(\text{S}_8\text{PcMg})]$.

nation to $\text{K}_8[\text{S}_8\text{PcMg}]$ has on the complexes' spectra, as this has never before been examined. Sn is known to form covalent bonds to S, and therefore the effect that Sn has on the overall energy of the transition was not expected to be as great as that of the group 10 metals. Additionally, the methyl groups of SnMe_3 should not participate strongly in the excited state dynamics. This was indeed the case, as can be seen in the absorption spectrum of $[(\text{Me}_3\text{Sn})_8(\text{S}_8\text{PcMg})]$ (Fig. 3), where the region of absorbance is approximately the same as that for $[(^{\text{Me}}\text{RS})_8\text{PcMg}]$. Of interest, though, is how the spectral profile has been significantly altered upon Sn coordination, and how the Q-band absorbance maximum has been both hypsochromically (blue-) shifted by 56 nm to 648 nm and at the same time reduced in strength to below that of the B-band. This unusual profile does somewhat resemble that of an aggregated Pc, but this could be ruled out during the determination of the molar absorption coefficient, where a linear response between concentration and absorbance was observed (see ESI, Fig. S2†). These changes suggest that the p-orbitals of the thiolates preferentially mix with the Me_3Sn groups rather than with the Pc π -system, giving a similar effect to β -alkoxy substitution.¹⁰

Like Sn, the coordination of diphosphino metal ions at the free thiolates of $\text{K}_8[\text{S}_8\text{PcMg}]$ causes several changes in the absorption spectra compared to $[(^{\text{Me}}\text{RS})_8\text{PcMg}]$, including the appearance of two new broad bands between the B- and Q-bands. However, unlike the Sn complex, it is the energy of the major features of the absorption spectra that are altered and not so much the profile. Most notably, the Q-band is strongly bathochromically (red-) shifted to 770, 765 and 764 nm for the Ni, Pd and Pt complexes, respectively. These values are very similar, and show that the nature of the metal ion has little effect on the HOMO–LUMO energy gap. The magnitude of the red-shift at *ca.* 70 nm is also greater than the observed red-shift of 50 nm seen for octathiolato-porphyrine complexes coordinated to diphosphino metal fragments prepared earlier.^{18f} The normalized absorption spectra of all metal-capped $[\text{S}_8\text{PcMg}]^{8-}$ complexes are shown in Fig. 3, and the absorbance maxima and their associated molar attenuation coefficients are given in Table 2.

Table 1 ^{31}P NMR chemical shifts (ppm) for the heteroleptic complexes $[(\text{dppeM})_4(\text{S}_8\text{PcMg})]$ and $[\text{M}(\text{dppe})(\text{dtpn})]$

Compound	^{31}P δ (ppm)	$^1J_{\text{Pt,P}}$ (Hz)
$[\text{Ni}(\text{dppe})(\text{dtpn})]$	60.1	—
$[(\text{dppeNi})_4(\text{S}_8\text{PcMg})]$	30.2	—
$[\text{Pd}(\text{dppe})(\text{dtpn})]$	53.2	—
$[(\text{dppePd})_4(\text{S}_8\text{PcMg})]$	53.3	—
$[\text{Pt}(\text{dppe})(\text{dtpn})]$	44.6	1399
$[(\text{dppePt})_4(\text{S}_8\text{PcMg})]$	48.3	1160

Table 2 Absorbance wavelength and molar attenuation coefficients measured in DMF

Complex	Wavelength/nm ($\epsilon/\text{dm}^3 \text{ mol}^{-1} \text{ cm}^{-1}$) ^{a,b}				
[(dppeNi) ₄ (S ₈ PcMg)]	770 (70 000)	700 (28 000) (sh)	534 (19 000) (br)	362 (51 000)	
[(dppePd) ₄ (S ₈ PcMg)]	765 (71 000)	698 (39 000) (sh)	580 (22 000) (br)	468 (24 000) (br)	354 (66 000)
[(dppePt) ₄ (S ₈ PcMg)]	764 (68 000)	702 (29 000) (sh)	559 (15 000) (br)	473 (18 000) (br)	360 (45 000)

^a sh denotes a shoulder on a larger peak. ^b br denotes a broad peak.

3.4. Singlet oxygen quantum yields

Although the identity of the coordinated transition metals made little difference on the absorption properties of the complexes, we were interested to see if they would have a different effect on the excited state dynamics. We therefore measured the rate of decay of the singlet oxygen quencher diphenylbenzofuran (DPBF) in the presence of the [(dppeM)₄(S₈PcMg)] complexes to indirectly determine the population of the T₁ state, and hence the amount of inter-system crossing (ISC), upon photoexcitation.

Fig. 4 shows the plot of $\ln(A_0/A_t)$ vs. time (s) for [(dppeM)₄(S₈PcMg)] (M = Ni, Pd, Pt) versus [Zn(py)(Pc)], which was used as the standard. All the metal–phosphine complexes show higher than usual singlet oxygen quantum yields (Φ_Δ) for Mg(Pc) complexes, which are known to be poor sensitizers for singlet oxygen production.²⁶ [(dppeNi)₄(S₈PcMg)] shows the lowest activity, which, at $\Phi_\Delta = 0.36$, is lower than that of [Zn(Py)(Pc)] (0.56 in DMF²²). [(dppePd)₄(S₈PcMg)] and [(dppePt)₄(S₈PcMg)], however, both show very high activity, with Φ_Δ values of 0.76 and 0.91, respectively.

Typically, [PcMg] and its derivatives have very low Φ_Δ values, which are ascribed to the inability of the Mg²⁺ ion to facilitate ISC through spin–orbit coupling of the S₁ and T₁ manifolds.²⁷ Additionally, it is known that diamagnetic heavy transition metals coordinated in the Pc cavity facilitate ISC through their d-orbitals. The heavier the metal, the greater the amount of ISC will be. This is often referred to as the heavy atom effect.²⁸ In the series synthesised here, the only difference between the complexes is the group 10 metal used, and therefore the higher Φ_Δ values can only be attributed to the

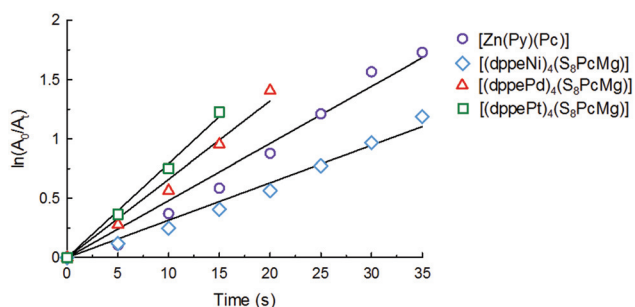


Fig. 4 Plot of $\ln(A_0/A_t)$ vs. time (s) for [(dppeNi)₄(S₈PcMg)], [(dppePd)₄(S₈PcMg)], [(dppePt)₄(S₈PcMg)] and [Zn(Py)(Pc)] determined from the decay of DPBF under irradiation by visible light of wavelengths >500 nm.

presence of diamagnetic heavier d⁸ M²⁺ ions. These results show that the metals peripherally coordinated through thiolate groups also interact with the Pc π -system to increase ISC. It is therefore possible that they could also be involved in other photophysical and photochemical processes of the Pc ligand.

3.5. MO calculations

TDDFT calculations were performed at the B3LYP/LANL2DZ level of theory on the optimized gas-phase structures for the complexes [(dppeNi)₄(S₈PcMg)], [(dppePd)₄(S₈PcMg)] and [(dppePt)₄(S₈PcMg)] to gain insight into how the coordination of the diphosphino metal ions affects the Pc's electronic properties; in particular, how the energy of the molecular orbitals (MOs) associated with complexes' absorption is altered. For comparison, a TDDFT calculation at the B3LYP/LANL2DZ level of theory was performed on the gas-phase optimized structure of Mg(octamethylthiophthalocyanine) [(MeS)₈PcMg]. [(MeS)₈PcMg] was chosen because it has an identical core structure to the studied complexes, but differs in the thiol groups that are methylated. For the simple complex [(MeS)₈PcMg], the calculation results match well with the four-orbital model of Gouterman,²⁹ where the HOMO is significantly more destabilized than the HOMO–1, and the LUMO and LUMO+1 are degenerate. Here, the transitions HOMO → LUMO/LUMO+1 give rise to the Q-band absorption.

Comparison of the metal-capped complexes to [(MeS)₈PcMg] shows that the formation of thiocatecholates and coordination of d⁸ metal ions cause a destabilization of both the HOMO and the degenerate LUMO/LUMO+1 by 1.7 eV and 1.5 eV for the Ni, 1.7 eV and 1.6 eV for the Pd, and 1.7 eV and 1.6 eV for the Pt complexes, respectively. The red-shift of the Q-band in these complexes arises because the HOMO is destabilised more than the LUMO by formation of the dithiolato metal heterocycle, which causes a narrowing of the band gap by about 0.12 eV. Calculations also predict what is observed by UV-Vis spectroscopy; that Ni, Pd, and Pt have almost the same amount of influence on the energy of the Q-band absorption. As expected, the Q-band transitions have mostly $\pi \rightarrow \pi^*$ characteristic. However, the LUMO/LUMO+1 are dispersed over both the macrocycle and the dithiocatecholate metal diphosphine moieties [S₂MP₂], so that there is also a small charge transfer contribution to the Q-band transitions. Additionally, the higher energy transitions associated with the new bands between 400 and 650 nm are predicted to be largely charge transfer processes between the isoindoline-dithiolate moieties and the peripheral [S₂MP₂] moieties. This is in

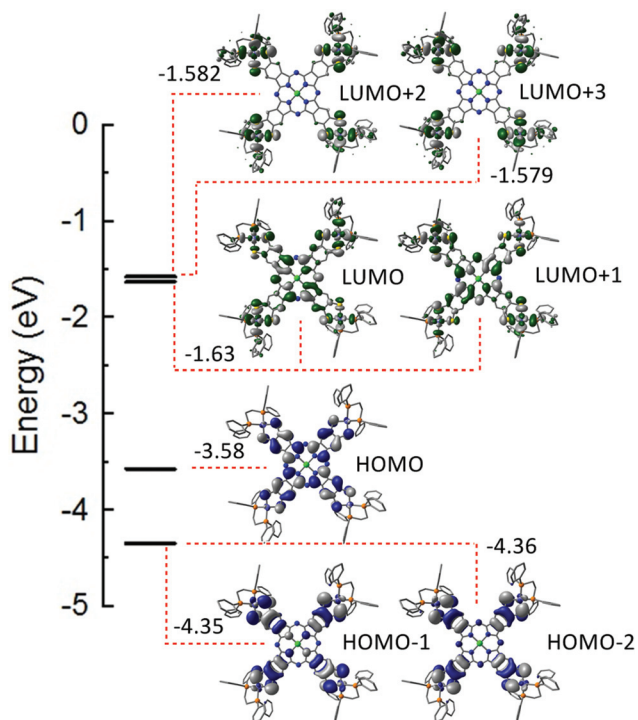


Fig. 5 Contour plots for HOMO–2 to LUMO+3 for [(dppeNi)₄(S₈PcMg)]. The Q-band transition involves MOs with mostly π/π^* characteristic, while the higher energy transitions are predominantly charge transfer processes.

Table 3 Calculated energies (eV) and wavelengths (nm) for the HOMO–LUMO transitions and their associated oscillator strengths (*f*) for the metal-capped and model complex studied

Complex	$\Delta(E_{\text{LUMO}} - E_{\text{HOMO}})$ (eV)	λ (nm)	<i>f</i>
[(dppeNi) ₄ (S ₈ PcMg)]	1.86	665.8	0.72
[(dppePd) ₄ (S ₈ PcMg)]	1.86	665.4	0.76
[(dppePt) ₄ (S ₈ PcMg)]	1.85	671.6	0.78
[(MeS) ₈ PcMg]	1.98	626.8	0.56

keeping with the well-known, good electron donating properties of dithiocatecholato ligand systems. Furthermore, while HOMO–1/–2 and LUMO+2/+3 are not strictly degenerate MOs, they are separated by only a small predicted energy difference of 0.01 eV and 0.003 eV, respectively. Contour plots for HOMO–2 to LUMO+3 and for [(dppeNi)₄(S₈PcMg)] as a representative example are shown in Fig. 5. The calculated transition energies (eV and nm) and oscillator strengths (*f*) for all pentanuclear complexes studied are given in Table 3.

4. Conclusions

We have demonstrated that the synthesis and cleavage of *S*-benzimidazolium groups is a mild, facile and viable option for introducing anionic thiolato and dithiocatecholato groups onto the Pc ligand scaffold and other aromatic systems. The

deprotection protocol under weakly basic conditions is compatible with the presence of Lewis acidic transition metal complex fragments, which act as scavengers for thiocatecholate. This offers new perspectives in coupling such chromophores with a variety of transition metals *via* thiocatecholate bridges. The coordination of group 10 metals significantly enhances the Pc ligand's absorption by inducing a strong red-shift of the Q-band to almost 800 nm. Additionally, the absorbance in the entire visible region is increased by the emergence of new broad bands between 400 and 650 nm, so that the metal-capped complexes display truly panchromatic absorbance. Along with this light absorption, the transition metal-capped complexes show a strong increase in their singlet oxygen quantum yields. Φ_{Δ} values increase in the order Ni > Pd > Pt, indicating that the heavy atom effect is clearly present, and, more importantly, that the peripheral metal ions interact with the Pc ligand's π -system and support ISC. This mixing is further supported by TDDFT calculations of the electronic transitions for the optimised structures of these complexes, which predict that the Q-band transitions have both $\pi \rightarrow \pi^*$ and CT characteristics. CT is proposed to be a result of the strong electron donor properties of the dithiocatecholato metal system. The strong red-shift observed is due to an increased destabilisation of the HOMO compared to the LUMO/LUMO+1 in the title compounds. Finally, the incorporation of an excellent chromophore, *viz.* PcMg, into a heteroleptic tetra-thiocatecholato complex both enhances the optical absorption of the chromophore and combines the strong absorbance of the Pc dye with the redox activity of metal thiocatecholato functionalities, thus opening perspectives for the design of photo-active complexes for energy transfer and photoredox catalysis. Analysis of their photo-redox chemistry will be the focus of further studies.

Conflicts of interest

There are no conflicts to declare.

Acknowledgements

MAB would like to thank the German Academic Exchange Service (DAAD) for a doctoral scholarship.

Notes and references

- (a) C. Browning, J. M. Hudson, E. W. Reinheimer, F.-L. Kuo, R. N. McDougald Jr., H. Raba , H. Pan, J. Bacs , X. Wang, K. R. Dunbar, N. D. Shepherd and M. A. Omary, *J. Am. Chem. Soc.*, 2014, **136**, 16185–16200; (b) C. L. Linfoot, P. Richardson, K. L. McCall, J. R. Durrant, A. Morandeira and N. Robertson, *Sol. Energy*, 2011, **85**, 1195–1203.
- (a) L. Gan, T. L. Groy, P. Tarakeshwar, S. K. S. Mazinani, J. Shearer, V. Mujica and A. K. Jones, *J. Am. Chem. Soc.*, 2015, **137**, 1109–1115; (b) K. E. Rosenkoetter, J. W. Ziller

- and A. F. Heyduk, *Inorg. Chem.*, 2016, **55**, 6794–6798;
- (c) P. Du and R. Eisenberg, *Energy Environ. Sci.*, 2012, **5**, 6012.
- 3 (a) J. M. Bevilacqua, J. A. Zuleteandand and R. Eisenberg, *Inorg. Chem.*, 1994, **33**, 258–266; (b) R. Benedix, D. Pitsch, K. Schone and H. Hennig, *Z. Anorg. Allg. Chem.*, 1986, **542**, 102–116; (c) R. L. Cowan, D. B. Pourreau, A. L. Rheingold, S. J. Geiband and W. C. Trogler, *Inorg. Chem.*, 1987, **26**, 259–265; (d) L. Gan, T. L. Groy, P. Tarakeshwar, S. K. S. Mazinani, J. Shearer, V. Mujica and A. K. Jones, *J. Am. Chem. Soc.*, 2015, **137**, 1109–1115.
- 4 S. D. Cummings and R. Eisenberg, *J. Am. Chem. Soc.*, 1996, **118**, 1949–1960.
- 5 D. Espa, L. Pilia, L. Marchiò, F. Artizzu, A. Serpe, M. L. Mercuri, D. Simão, M. Almeida, M. Pizzotti, F. Tessore and P. Deplano, *Dalton Trans.*, 2012, **41**, 3485.
- 6 B. Zheng, R. P. Sabatini, W.-F. Fu, M. S. Eum, W. W. Brennessel, L. Wang, D. W. McCamantand and R. Eisenberg, *Proc. Natl. Acad. Sci. U. S. A.*, 2015, E3987–E3996.
- 7 D. Wöhrle, G. Schnurpfeil, S. Makarovand and O. Suvora, *Chem. Unserer Zeit*, 2012, **46**, 12–24.
- 8 (a) L. Martin-Gomis, F. Fernández-Lázaro and A. Sastre-Santos, *J. Mater. Chem. A*, 2014, **2**, 15672–15682; (b) X. Zhang, T. Peng and S. Song, *J. Mater. Chem. A*, 2016, **4**, 2365–2402.
- 9 C. K. C. Bikram, N. K. Subbaiyan and F. D'Souza, *J. Phys. Chem. C*, 2012, **116**, 11964–11972.
- 10 T. Kawata, Y. Chino, N. Kobayashi and M. Kimura, *Langmuir*, 2018, **34**, 7294–7300.
- 11 X.-F. Chen, M. E. El-Khouly, K. Ohkubo, S. Fukuzumi and D. K. P. Ng, *Chem. – Eur. J.*, 2018, **24**, 3862–3872.
- 12 J. Fernandez-Ariza, M. Urbani, M. S. Rodriguez-Morgade and T. Torres, *Chem. – Eur. J.*, 2018, **24**, 2618–2625.
- 13 J. Demuth, R. Kucera, K. Kopecky, Z. Havlinova, A. Libra, V. Novakova, M. Miletin and P. Zimčík, *Chem. – Eur. J.*, 2018, **24**, 9658–9666.
- 14 E. A. Ermilov, J.-Y. Liu, R. Menting, Y.-S. Huang, B. Röding and D. K. P. Ng, *Phys. Chem. Chem. Phys.*, 2016, **18**, 10964–10975.
- 15 N. Kobayashi, H. Ogata, N. Nonaka and E. A. Luk'yanets, *Chem. – Eur. J.*, 2003, **9**, 5123–5134.
- 16 T. Furuyama, K. Satoh, T. Kushiya and N. Kobayashi, *J. Am. Chem. Soc.*, 2014, **136**, 765–776.
- 17 (a) T. Kimura, A. Yomogita, T. Matsutani, T. Suzuki, I. Tanaka, Y. Kawai, Y. Takaguchi, T. Wakahara and T. Akasaka, *J. Org. Chem.*, 2004, **69**, 4716–4473.
- 18 (a) C. S. Velázquez, W. E. Broderick, M. Sabat, A. G. M. Barrett and B. M. Hoffman, *J. Am. Chem. Soc.*, 1990, **112**, 7408–7410; (b) T. F. Baumann, J. W. Sibert, M. M. Olmstead, A. G. M. Barrett and B. M. Hoffman, *J. Am. Chem. Soc.*, 1994, **116**, 2639–2640; (c) S. L. J. Michel, D. P. Goldberg, C. Stern, A. G. M. Barrett and B. M. Hoffman, *J. Am. Chem. Soc.*, 2001, **123**, 4741–4748;
- (d) T. F. Baumann, M. S. Nasir, J. W. Sibert, A. J. P. White, M. M. Olmstead, D. J. Williams, A. G. M. Barrett and B. M. Hoffman, *J. Am. Chem. Soc.*, 1996, **118**, 10479–10486;
- (e) J. W. Sibert, T. F. Baumann, D. J. Williams, A. J. P. White, A. G. M. Barrett and B. M. Hoffman, *J. Am. Chem. Soc.*, 1996, **118**, 10487–10493; (f) C. S. Velázquez, T. F. Baumann, M. M. Olmstead, H. Hope, A. G. M. Barrett and B. M. Hoffman, *J. Am. Chem. Soc.*, 1993, **115**, 9997–10003.
- 19 (a) J. M. Tour, L. Jones II, D. L. Pearson, J. J. S. Lamba, T. P. Burgin, G. M. Whitesides, D. L. Allara, A. N. Parikh and S. V. Atre, *J. Am. Chem. Soc.*, 1995, **117**, 9529–9534; (b) L. Cai, Y. Yao, J. Yang, D. W. Price Jr. and J. M. Tour, *Chem. Mater.*, 2002, **14**, 2905–2909.
- 20 D. Wöhrle, M. Eskes, K. Shigehara and A. Yamada, *Synthesis*, 1992, 194–196.
- 21 T. S. Zhivotova, A. M. Gazaliev, S. D. Fazylov, Z. K. Aitpaeva and D. M. Turdybekov, *Russ. J. Org. Chem.*, 2006, **42**, 448–450.
- 22 D. Çakir, M. Göksel, V. Çakir, M. Durmuş, Z. Biyikhoğlu and H. Kantekin, *Dalton Trans.*, 2015, **44**, 9646–9658.
- 23 W. Spiller, H. Kliesch, D. Wöhrle, S. Hackbarth, B. Roder and G. Schnurpfeil, *J. Porphyrins Phthalocyanines*, 1998, **2**, 145–158.
- 24 M. J. Frisch, G. W. Trucks, H. B. Schlegel, G. E. Scuseria, M. A. Robb, J. R. Cheeseman, G. Scalmani, V. Barone, B. Mennucci, G. A. Petersson, H. Nakatsuji, M. Caricato, X. Li, H. P. Hratchian, A. F. Izmaylov, J. Bloino, G. Zheng, J. L. Sonnenberg, M. Hada, M. Ehara, K. Toyota, R. Fukuda, J. Hasegawa, M. Ishida, T. Nakajima, Y. Honda, O. Kitao, H. Nakai, T. Vreven, J. A. Montgomery Jr., J. E. Peralta, F. Ogliaro, M. Bearpark, J. J. Heyd, E. Brothers, K. N. Kudin, V. N. Staroverov, T. Keith, R. Kobayashi, J. Normand, K. Raghavachari, A. Rendell, J. C. Burant, S. S. Iyengar, J. Tomasi, M. Cossi, N. Rega, J. M. Millam, M. Klene, J. E. Knox, J. B. Cross, V. Bakken, C. Adamo, J. Jaramillo, R. Gomperts, R. E. Stratmann, O. Yazyev, A. J. Austin, R. Cammi, C. Pomelli, J. W. Ochterski, R. L. Martin, K. Morokuma, V. G. Zakrzewski, G. A. Voth, P. Salvador, J. J. Dannenberg, S. Dapprich, A. D. Daniels, O. Farkas, J. B. Foresman, J. V. Ortiz, J. Cioslowski and D. J. Fox, *Gaussian 09, Revision C.01*, Gaussian, Inc., Wallingford CT, 2010.
- 25 N. Kobayashi, H. Ogata, N. Nonaka and E. A. Luk'yanets, *Chem. – Eur. J.*, 2003, **9**, 5123–5134.
- 26 M. Kostka, P. Zimcik, M. Miletin, P. Klemra, K. Kopecky and Z. Musil, *J. Photochem. Photobiol., A*, 2006, **178**, 16–25.
- 27 M. Kostka, P. Zimcik, M. Miletin, P. Klemra, K. Kopecky and Z. Musil, *J. Photochem. Photobiol., A*, 2006, **178**, 16–25.
- 28 P. S. Vincett, E. M. Voigt and K. E. Rieckhoff, *J. Chem. Phys.*, 1971, **55**, 4131–4140.
- 29 C. Weiss, H. Kobayashi and M. Gouterman, *J. Mol. Spectrosc.*, 1965, **16**, 415–450.